AD

TECHNICAL REPORT ARCCB-TR-88037

FINITE ELEMENT ANALYSIS OF THE SWAGE AUTOFRETTAGE PROCESS

PETER C. T. CHEN

SEPTEMBER 1988

US ARMY ARMAMENT RESEARCH,
DEVELOPMENT AND ENGINEERING CENTER
CLOSE COMBAT ARMAMENTS CENTER
BENÉT LABORATORIES
WATERVLIET, N.Y. 12189-4050

APPROVED FOR PUBLIC RELEASE; DISTRIBUTION UNLIMITED

DISCLAIMER

The findings in this report are not to be construed as an official Department of the Army position unless so designated by other authorized documents.

The use of trade name(s) and/or manufacturer(s) does not constitute an official indorsement or approval.

DESTRUCTION NOTICE

For classified documents, follow the procedures in DoD 5200.22-M, Industrial Security Manual, Section II-19 or DoD 5200.1-R, Information Security Program Regulation, Chapter IX.

For unclassified, limited documents, destroy by any method that will prevent disclosure of contents or reconstruction of the document.

For unclassified, unlimited documents, destroy when the report is no longer needed. Do not return it to the originator.

SECURITY CLASSIFICATION OF THIS PAGE (When Data Entered)

REPORT DOCUMENTATION PAGE

READ INSTRUCTIONS BEFORE COMPLETING FORM

1. REPORT NUMBER: ARCCB-TR-88037	2. GOVT ACCESSION NO.: AD-A206-111
3. RECIPIENT'S CATALOG NUMBER	
4. TITLE (and Subtitle): FINITE ELEMENT ANALYSIS OF THE SWAGE AUTOFRETTAGE PROCESS	5. TYPE OF REPORT & PERIOD COVERED: Final
	6. PERFORMING ORG. REPORT NUMBER
7. AUTHOR(s): Peter C. T. Chen	8. CONTRACT OR GRANT NUMBER(s)
9. PERFORMING ORGANIZATION NAME AND ADDRESS: US Army ARDEC, Benet Laboratories, SMCAR-CCB-TL, Watervliet, NY 12189-4050	10. PROGRAM ELEMENT, PROJECT, TASK AREA & WORK UNIT NUMBERS: AMCMS No. 6126.23.1BL0.0, PRON No. 1A82.K24NMSC
11. CONTROLLING OFFICE NAME AND ADDRESS: US Army ARDEC, Close Combat Armaments Center, Picatinny Arsenal, NJ 07806-5000	12. REPORT DATE: September 1988
	13. NUMBER OF PAGES: 19
14. MONITORING AGENCY NAME & ADDRESS (if different from Controlling Office)	15. SECURITY CLASS. (of this report): UNCLASSIFIED
	15a. DECLASSIFICATION/DOWNGRADING SCHEDULE

16. DISTRIBUTION STATEMENT (of this Report)

Approved for public release; distribution unlimited.

17. DISTRIBUTION STATEMENT (of the abstract entered in Block 20, if different from Report)

18. SUPPLEMENTARY NOTES

Presented at the Sixth Army Conference on Applied Mathematics and Computing, University of Colorado, Boulder, CO, 31 May - 3 June 1988.
Published in Proceedings of the Conference.

19. KEY WORDS (Continue on reverse side if necessary and identify by block number)

Gun Tube; Residual Stress;
Autofrettage; Plasticity;
Swaging; Finite Element Analysis.

20. ABSTRACT (Continue on reverse side if necessary and identify by block number)

The swage autofrettage process is often used to produce favorable residual stresses in a tube. In this report a finite element analysis of the swage autofrettage process is presented. The nonlinear finite element program (ABAQUS) is used to obtain numerical results for the displacements, strains, and stresses in the tube during and after autofrettage. Approximate solutions are obtained for one- and two-dimensional tubes pressed by rigid or elastic mandrels. The longitudinal effect and the elasticity of the mandrel on the permanent bore enlargement and the residual stresses are discussed.

DD FORM 1 JAN 73 1473 EDITION OF 1 NOV 65 IS OBSOLETE

UNCLASSIFIED

SECURITY CLASSIFICATION OF THIS PAGE (When Data Entered)

TABLE OF CONTENTS

TABLES

LIST OF ILLUSTRATIONS

A-1

INTRODUCTION

To increase the maximum elastic carrying capacity and to enhance the fatigue life, residual stresses are often produced in tubes through autofrettage (ref 1). Many solutions are reported for the hydraulic autofrettage process. The thick-walled cylinders are subjected to uniform internal pressure of sufficient magnitude to cause plastic deformation and then the pressure is removed.

A more economical way of producing residual stresses in thick-walled cylinders is the swage autofrettage process. This process is carried out by a mandrel, the diameter of which is greater than the inner diameter of the tube. The mandrel is driven through the tube from one end to the other. A rigorous analysis of this process is difficult. However, recently a simple analysis of the swage autofrettage process was reported (ref 2). The model used was a simplified plane-strain problem of the mandrel-tube assembly. The steel tube was assumed to be elastically-ideally plastic, obeying Tresca's yield criterion and the associated flow theory, but the tungsten carbide mandrel was elastic. The deformation and stress distribution during swaging were obtained by solving the shrink-fit problem beyond the elastic limit. After swaging, the permanent bore enlargement and residual stresses were calculated by an unloading analysis (ref 2), taking into account the Bauschinger effect and the strain-hardening during unloading (ref 3).

The solution reported in Reference 2 is in closed-form and the numerical results indicate that the agreement between the calculated and experimental data is excellent in zones with larger wall ratios but not so good in zones with wall ratios less than two. The differences in thinner sections may be due to the

---

References are listed at the end of this report.

longitudinal bending effect since the simplified analytical analysis is one-dimensional and bending is neglected. In order to determine the longitudinal effect, a two-dimensional analysis based on the finite element method has been conducted. In this report, the finite element solutions are presented for both one- and two-dimensional models and a comparison of the results is given.

METHOD OF ANALYSIS

Since the total length of the tube is about sixty times the diameter of the mandrel, a complete finite element analysis of the swage autofrettage process is very difficult. As the mandrel is driven through the tube from one end to the other, the simulation requires the study of elastic-plastic moving contact and separation history between two deforming bodies. In addition, considerable amounts of computer storage and run time are required. In the present study, however, approximate finite element models were chosen to represent swaging in only a part of the tube (zone 3). We consider the process as quasi-static and neglect the effect of sliding and friction between the mandrel and tube. We want to obtain the information about the deformations and stresses for a section at only two particular stages, i.e., when the mandrel is at or far away from the position of interest. To achieve this purpose, we can simplify the simulation by studying two related problems, i.e., shrink-fit and complete unloading.

When the mandrel is at the position of interest, we consider a shrink-fit problem of the mandrel-tube assembly to obtain the maximum deformation and stresses during swaging. When the mandrel is driven far away from the section, we study it as a complete unloading problem of the mandrel-tube assembly to obtain the information about the permanent bore enlargement and residual stresses after swaging. Figure 1 shows a one-dimensional interference-fit

problem of the mandrel-tube assembly. Initially, the inner and outer radii of the tube are a and b and the radius of the mandrel is c. Given the interference I = c-a, we can determine the interference pressure p and the deformation and stresses in the mandrel and tube. In general, this problem can be solved only by an iterative approach. If the mandrel were rigid, then the direct approach using displacement constraints could be applied. The results based on this approach were obtained so we could discuss the effect of elasticity in the mandrel. The actual strength ratio of tungsten carbide to steel is about three. For the problem considered here, it is reasonable to assume that the steel tube is elastic-plastic, obeying Mises' yield criterion and the associated flow theory, but the tungsten carbide mandrel remains elastic. The finite element analysis is carried out by using the nonlinear program, ABAQUS (ref 4). Two types of elements used are shown in Figure 2. The axisymmetric solid elements (CAX4) are used to model the tube and mandrel. The interface elements (INTER2A) are used to model the separation or interference fit between the mandrel and tube. Truss elements (CID2) can also be used to model the mandrel because the displacement U_1 is directly related to the external pressure p by

$$U_1/c = -(1-\nu_1-2\nu_1^2)p/E$$

where E_1, ν_1 are elastic constants of the mandrel.

FINITE ELEMENT MODEL

Figure 3 shows a two-dimensional finite element model (E3) chosen to represent the swaging process in zone 3. The model is considered symmetric with respect to z = 0 so that only half of the model is shown. We have used 133 and 21 elements of type CAX4 to represent the tube and mandrel, respectively, with a = 1, b = 1.431, c = 1.007415. There are eight interface elements of type

INTER2A to represent the interaction between the tube and mandrel. Figure 3a shows an interference-fit problem of the mandrel-tube assembly. This model is used to determine the maximum deformation and stresses during swaging. Figure 3b shows a complete unloading problem when the two parts are separated. This problem is used to determine the permanent deformation and residual stresses after swaging. In order to determine the longitudinal bending effect, we would like to compare the two-dimensional analysis with the one-dimensional analysis. The one-dimensional model (E1) consists of ten elements (of type CAX4) each for the tube and mandrel with one interface element (of type INTER2A). Another one-dimensional model (E2) has the mandrel represented by one or two truss elements of type CID2. The material constants used are $E = 200$, $\sigma_o = 1$, $\nu = 0.3$ for the high strength steel and $E_1 = 590$, $\sigma_1 = 3.33$, $\nu_1 = 0.258$ for the tungsten carbide. The materials exhibit no strain-hardening. In the modeling and computation we have used the dimensionless quantities with the inner radius (2.283 inches) as the unit length and the initial yield stress (150 Ksi) as the unit stress. The actual quantities can be obtained easily if needed.

In the above three models (E1, E2, E3), the tube is elastic-plastic, but the mandrel remains elastic. If the strength ratio of the mandrel material to tube material is very large, then the mandrel can be regarded as rigid. In order to determine the effect of elasticity in the mandrel, we have chosen three finite element models (R1, R2, R3). Models R1 and R2 represent one-dimensional plane-strain and plane-stress cases, respectively. We have used ten elements of type CAX4 to represent the tube. The model R3 is the same as the model E3 shown in Figure 3 except that the mandrel is replaced by a rigid block.

Following the instructions given in Reference 4, we have prepared the input data for each of the six finite element models. For each model we ran the

problem in two steps, i.e., loading and unloading. The input deck for the finite element analysis of model E1 is shown in Table I.

RESULTS AND DISCUSSIONS

For each of the six models (R1, R2, R3, E1, E2, E3) discussed in the preceding section, we have run the finite element program successfully. The numerical results for the displacements, strains, and stresses in the tube during and after swaging have been obtained. Only the results for the stresses along the radial direction near $z = 0$ and the displacements along the bore are presented graphically.

When the mandrel is assumed to be rigid, the displacement at the bore is equal to the given interference. The results for the stresses based on models (R1, R2, R3) are presented in Figures 4 through 6. When the interference is only half of the maximum, the state of stresses remains elastic as shown in Figures 4 and 5. When the maximum interference ($I = 0.007415$) is reached, the state of stresses is elastic-plastic. The effect of interference on the distributions of hoop and axial stresses can be seen in Figures 4 and 5, respectively. By comparing the results for model R1 (one-dimensional, plane-strain case) and model R3 (two-dimensional case), we can also see the influence of the longitudinal effect on the hoop and axial stresses. The influence on the maximum axial stresses is very significant as shown in Figure 5. Unloading after the maximum interference is reached, we have obtained the residual stresses as shown in Figures 5 and 6 for the axial and hoop stresses. A comparison of these residual stresses indicates that the differences between one- and two-dimensional models (R1 and R3) are very minor. Models R1 and R2 represent plane-strain and plane-stress cases, respectively, and both models are one-dimensional.

When the mandrel is considered as elastic, the interference-fit assembly is solved iteratively. The same results for the one-dimensional models (E1 and E2) have been obtained. A comparison of two models (E1 and R1) for the hoop stresses during and after swaging is shown in Figure 7. The elasticity in the mandrel reduces the amount of overstrain from 70 to 60 percent. The numerical results for the two-dimensional model (E3) are presented in Figures 8 through 11. Figure 8 shows the distributions of hoop stresses during and after swaging. Figure 9 shows the corresponding distributions of maximum and residual axial stresses. Also shown in Figures 8 and 9 are the one-dimensional results based on model E1. A comparison of the results based on models E1 and E3 can determine the two-dimensional effect on these stresses. In Figure 10 we show the results for the radial stresses based on four models (E1, E3, R1, R3). Finally, the results based on several models for the radial displacement along the bore are presented in Figure 11. The displacements during and after swaging are represented by U and U", respectively. Also shown in the figure is the measured permanent bore enlargement. By comparing the results based on models E1 and R1, the elasticity effect gives a smaller value for U". If we include the two-dimensional effect with model E3, we get a value for U" even smaller than that based on the one-dimensional model.

REFERENCES

1. Davidson, T. E. and Kendall, D. P., "The Design of Pressure Vessels for Very High Pressure Operation," Mechanical Behavior of Materials Under Pressure, (H.Ll.P. Pugh, ed.), Elsevier Co., 1970.

2. Chen, P. C. T., "A Simple Analysis of the Swage Autofrettage Process," Transactions of the Fifth Army Conference on Applied Mathematics and Computing, ARO Report 88-1, Research Triangle Park, NC, March 1988, pp. 149-159.

3. Milligan, R. V., Koo, W. H., and Davidson, T. E., "The Bauschinger Effect in a High Strength Steel," Journal of Basic Engineering, Vol. 88, 1966, pp. 480-488.

4. "ABAQUS Users' Manual," Version 4.6, Hibbit, Karlsson, and Sorensen, Inc., 1987.

TABLE I. THE FINITE ELEMENT INPUT DECK FOR MODEL E1

```
*HEADING
TUBE-MANDREL ASSEMBLY AND SEPARATION
*NODE
1,.
11,1.007415
21,1.0
31,1.431
101,.        , 0.05
111,1.007415, 0.05
121,1.0      , 0.05
131,1.431    , 0.05
*NGEN,NSET=SIDE1
1,11
101,111
*NGEN,NSET=SIDE2
21,31
121,131
*NSET,NSET=BORE
1,101
*ELEMENT,TYPE=CAX4
1,1,2,102,101
11,21,22,122,121
*ELGEN,ELSET=MANDREL
11,10
*ELGEN,ELSET=TUBE
11,10
*SOLID SECTION,ELSET=MANDREL,MATERIAL=CARBIDE
*MATERIAL,NAME=CARBIDE
*ELASTIC
590., .258
*PLASTIC
3.33
*SOLID SECTION,ELSET=TUBE,MATERIAL=STEEL
*MATERIAL,NAME=STEEL
*ELASTIC
2.E2, .3
*PLASTIC
1.
*ELEMENT,TYPE=INTER2A,ELSET=SFIT
101,111,11,121,21
*INTERFACE,ELSET=SFIT
*FRICTION
 .0
*BOUNDARY
SIDE1,2
SIDE2,2
*STEP, NLGEOM,CYCLE=10
*STATIC,PTOL=1.E-4,DIRECT
1. , 1.
*END STEP
*STEP,NLGEOM
*STATIC,PTOL=1.E-4 ,DIRECT
1.,1.
*MODEL CHANGE, REMOVE
MANDREL,SFIT
*END STEP
```

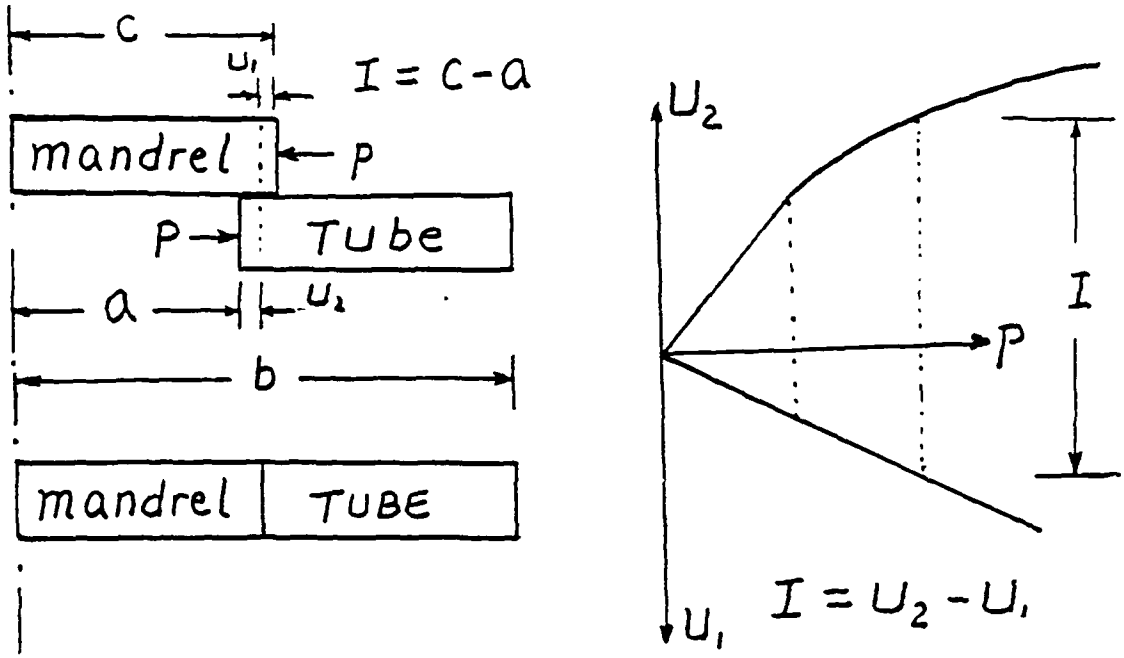

Figure 1. One-dimensional interference-fit assembly.

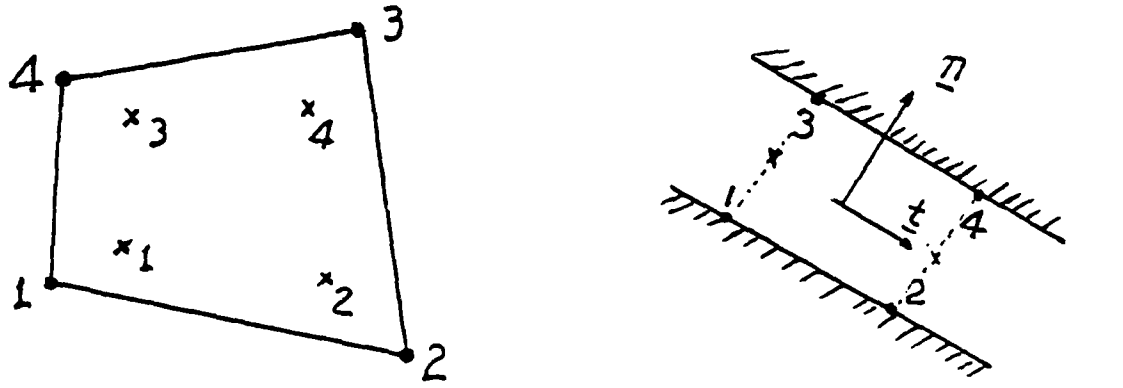

(a) solid element (CAX4)

(b) interface element (INTER2A)

Figure 2. Axisymmetric solid and interface elements.

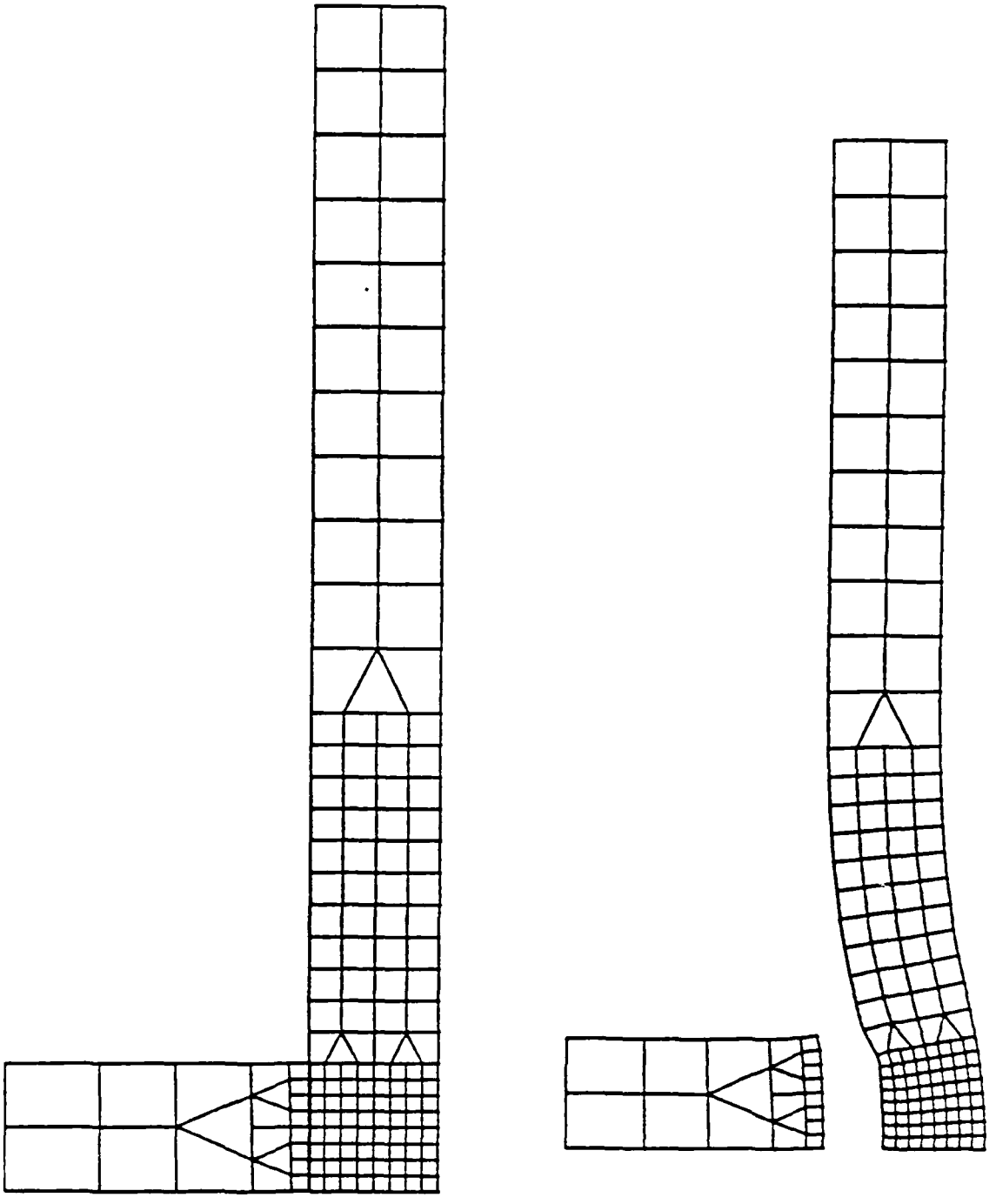

(a) interference-fit (b) separation

Figure 3. A two-dimensional finite element model.

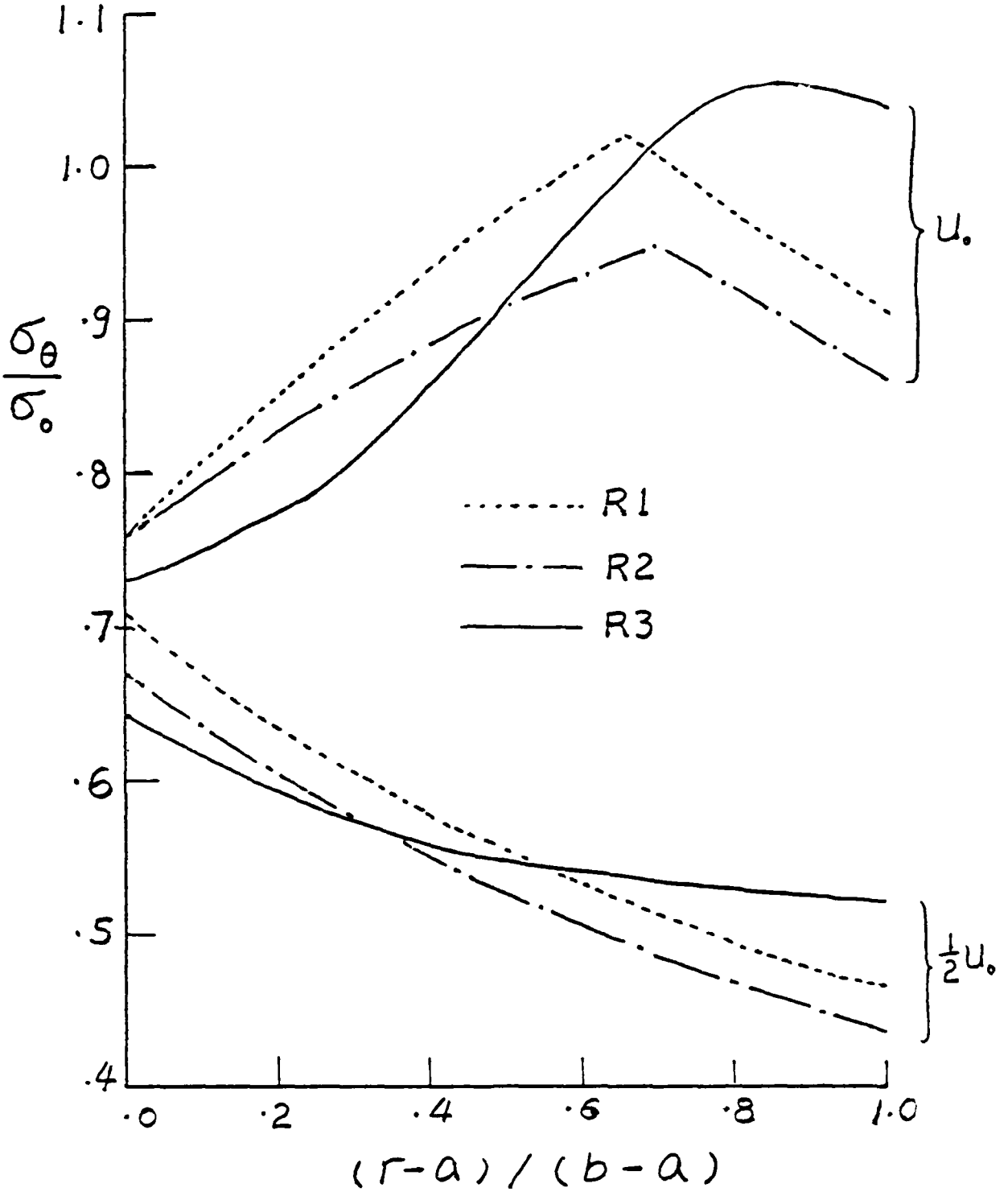

Figure 4. The effect of interference on the hoop stresses using rigid mandrels.

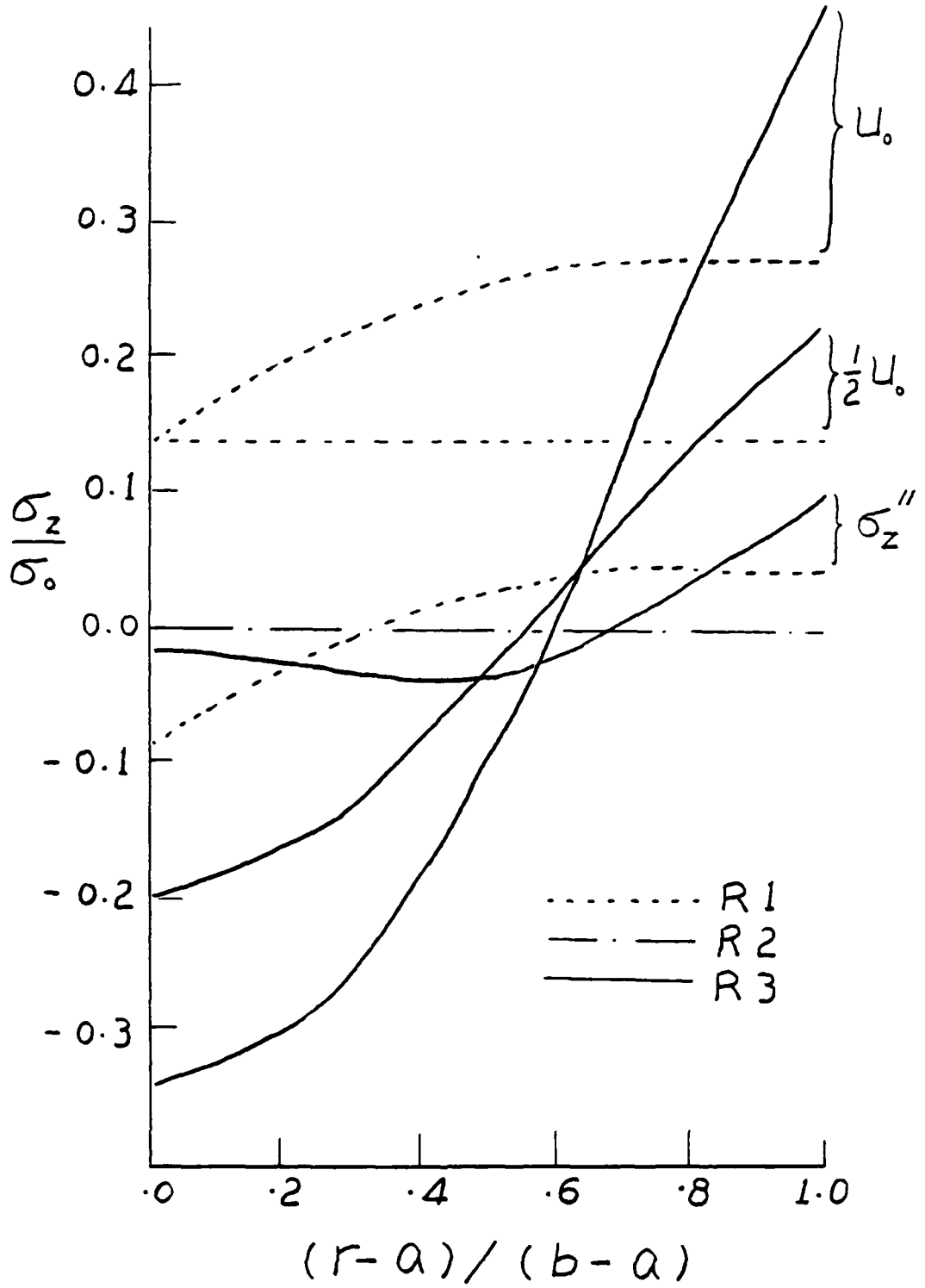

Figure 5. The effect of interference on the axial stresses using rigid mandrels.

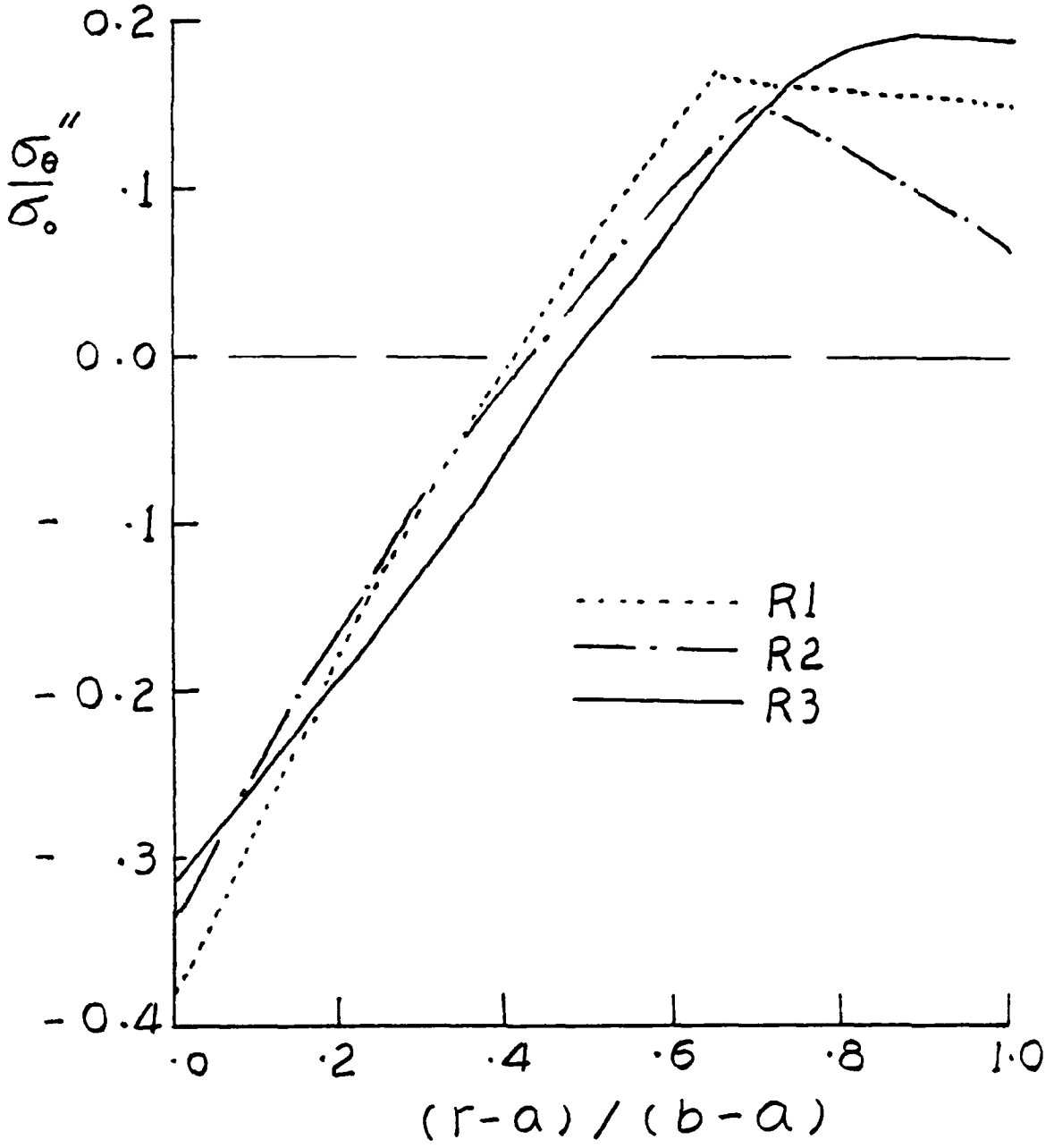

Figure 6. The effect of three rigid mandrels on the residual hoop stresses.

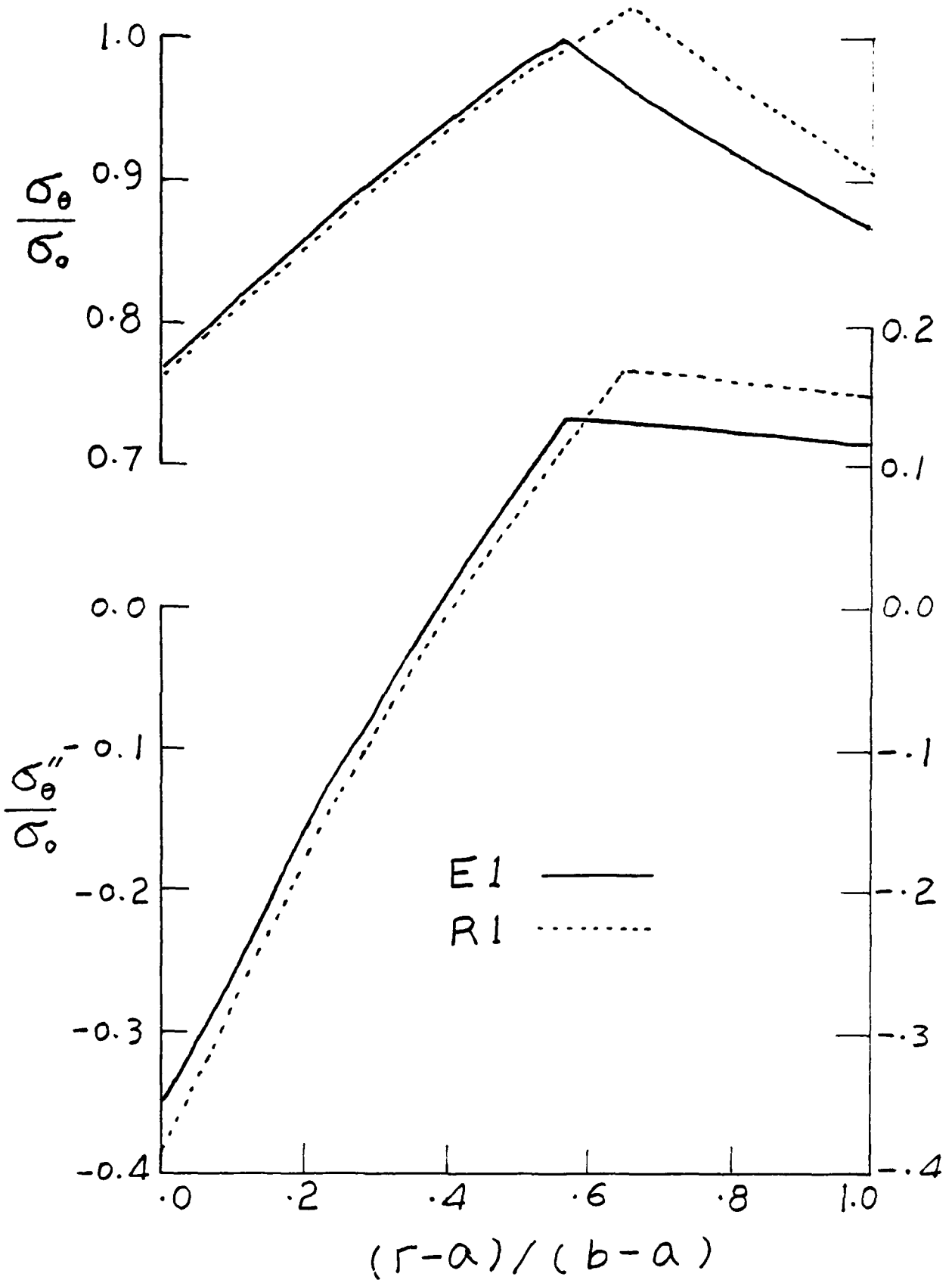

Figure 7. The effect of elasticity in the mandrel on the residual hoop stresses.

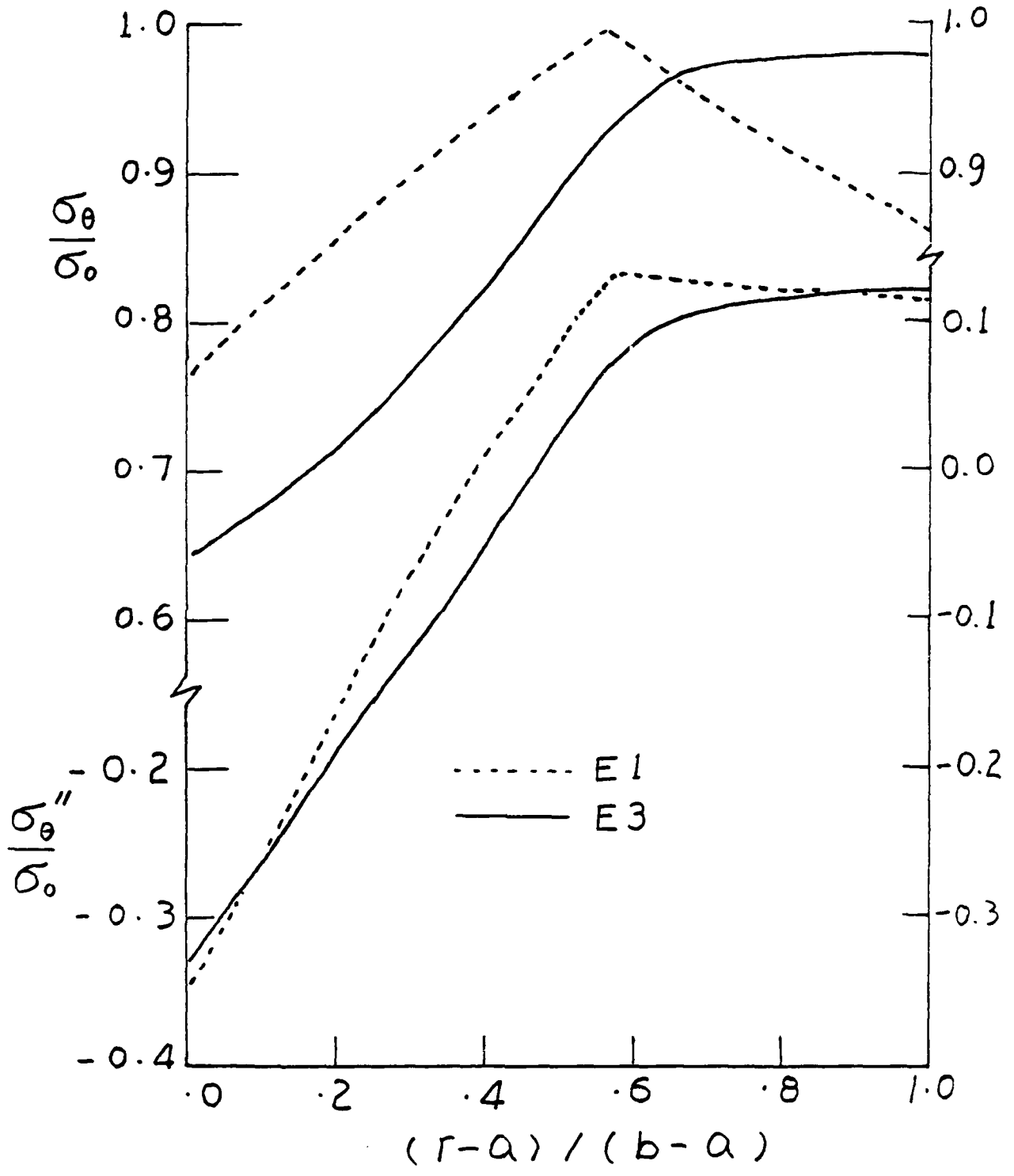

Figure 8. The two-dimensional effect of the mandrel on the residual hoop stresses.

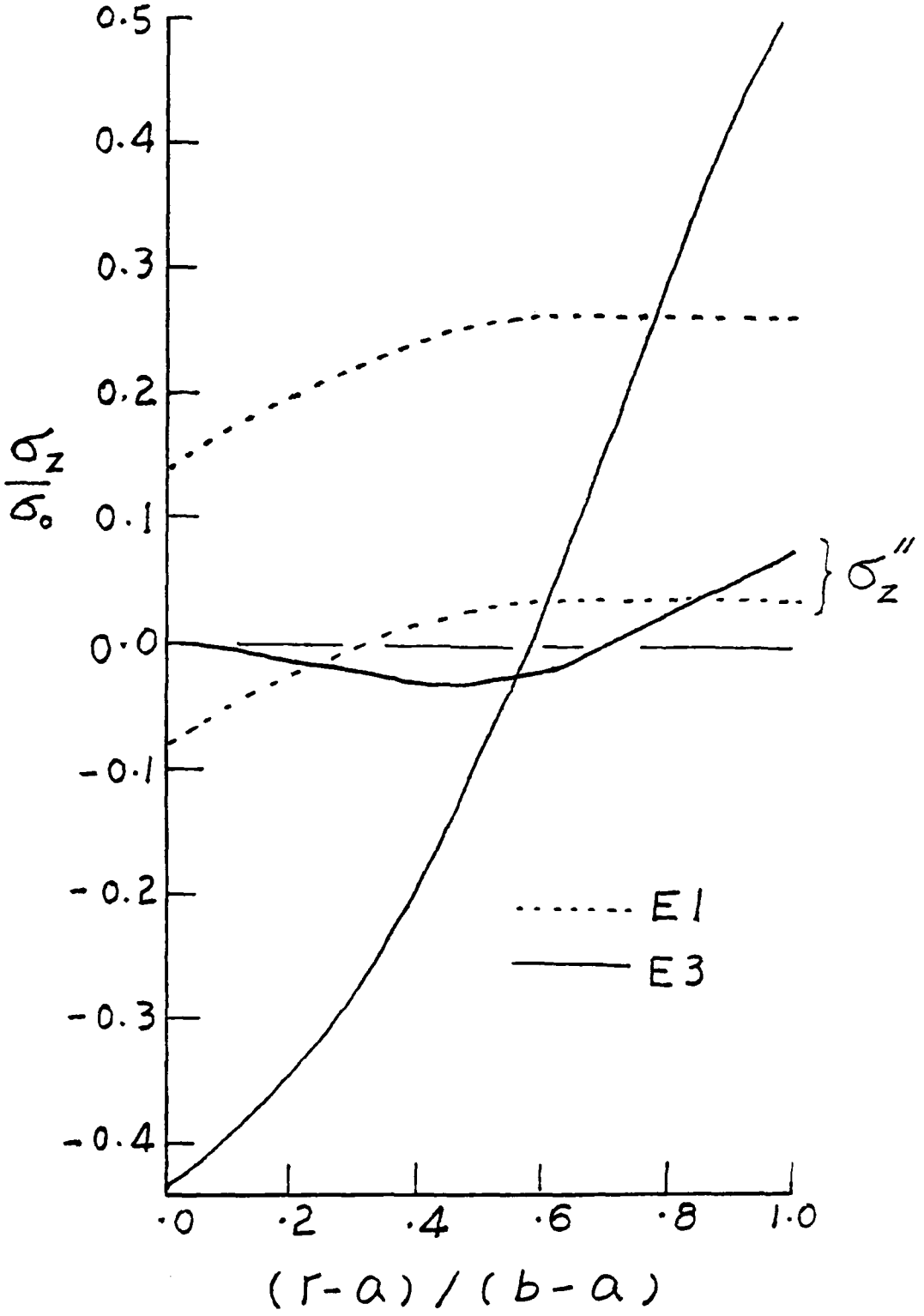

Figure 3. The two-dimensional effect of the mandrel on the axial stresses.

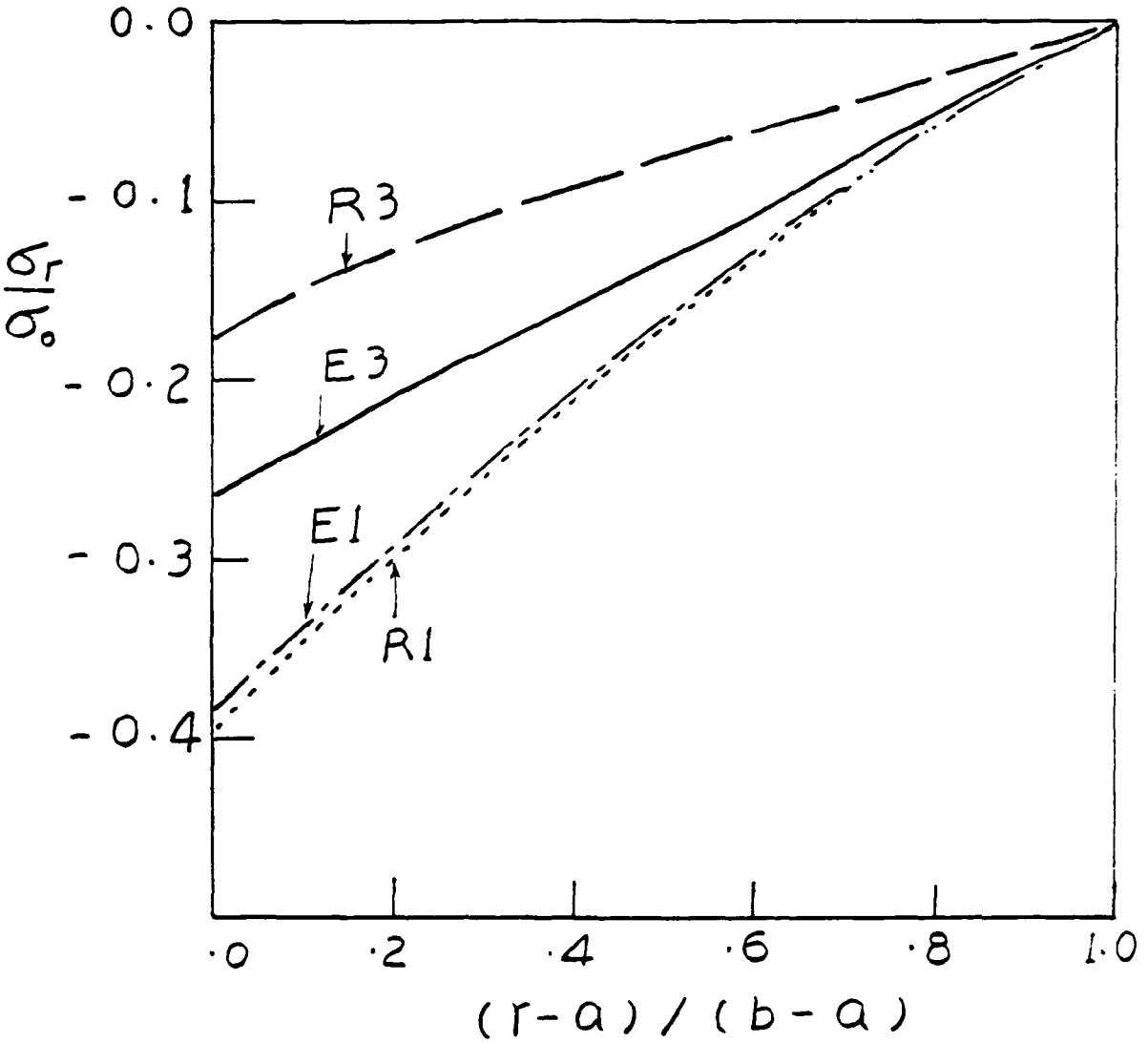

Figure 10. A comparison of radial stresses for four models.

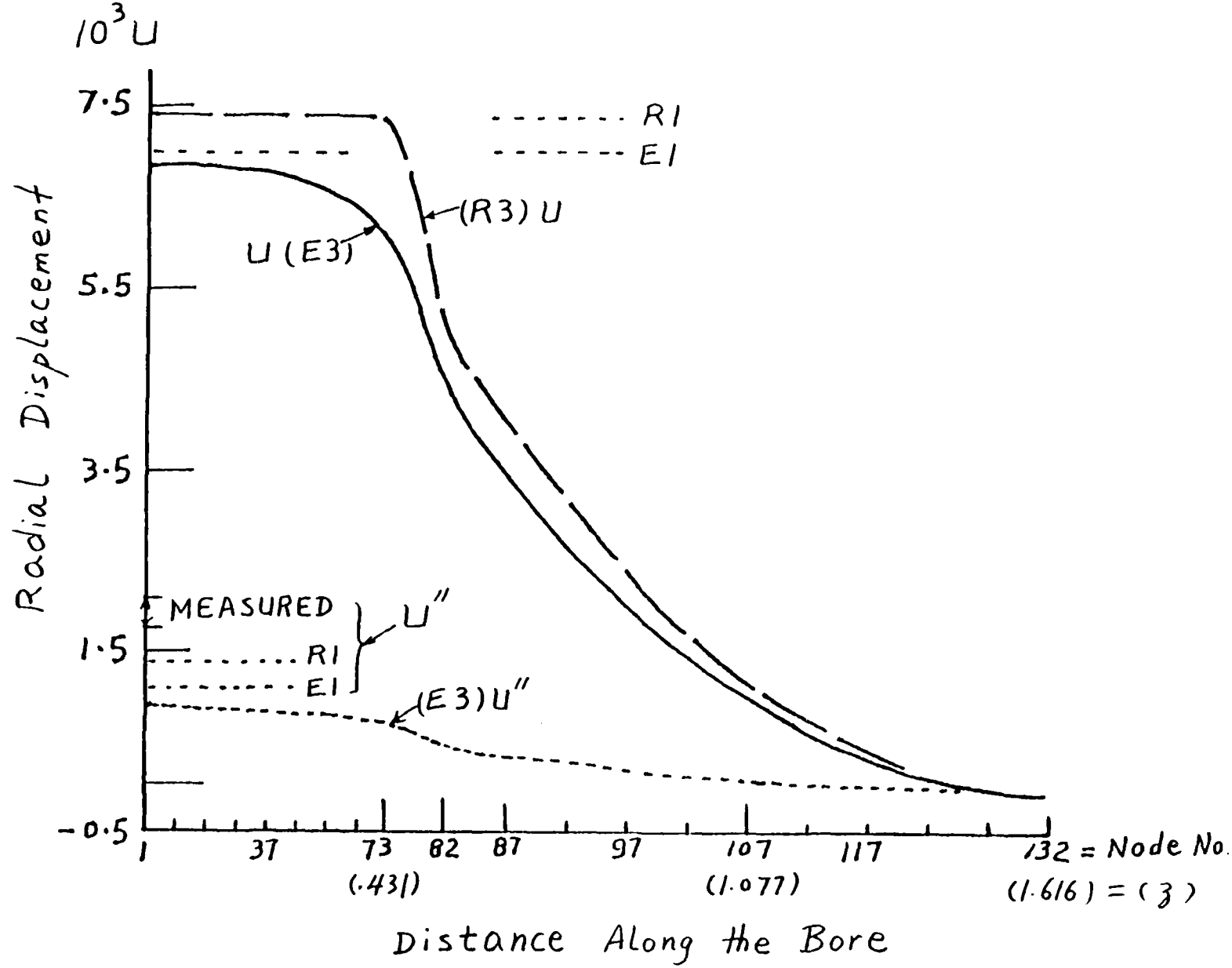

Figure 11. Radial displacements along the bore.

TECHNICAL REPORT INTERNAL DISTRIBUTION LIST

	NO. OF COPIES
CHIEF, DEVELOPMENT ENGINEERING BRANCH	
ATTN: SMCAR-CCB-D	1
-DA	1
-DC	1
-DM	1
-DP	1
-DR	1
-DS (SYSTEMS)	1
CHIEF, ENGINEERING SUPPORT BRANCH	
ATTN: SMCAR-CCB-S	1
-SE	1
CHIEF, RESEARCH BRANCH	
ATTN: SMCAR-CCB-R	2
-RA	1
-RM	1
-RP	1
-RT	1
TECHNICAL LIBRARY	5
ATTN: SMCAR-CCB-TL	
TECHNICAL PUBLICATIONS & EDITING UNIT	3
ATTN: SMCAR-CCB-TL	
DIRECTOR, OPERATIONS DIRECTORATE	1
ATTN: SMCWV-OD	
DIRECTOR, PROCUREMENT DIRECTORATE	1
ATTN: SMCWV-PP	
DIRECTOR, PRODUCT ASSURANCE DIRECTORATE	1
ATTN: SMCWV-QA	

NOTE: PLEASE NOTIFY DIRECTOR, BENET LABORATORIES, ATTN: SMCAR-CCB-TL, OF ANY ADDRESS CHANGES.

TECHNICAL REPORT EXTERNAL DISTRIBUTION LIST

	NO. OF COPIES
ASST SEC OF THE ARMY RESEARCH AND DEVELOPMENT ATTN: DEPT FOR SCI AND TECH THE PENTAGON WASHINGTON, D.C. 20310-0103	1
ADMINISTRATOR DEFENSE TECHNICAL INFO CENTER ATTN: DTIC-FDAC CAMERON STATION ALEXANDRIA, VA 22304-6145	12
COMMANDER US ARMY ARDEC ATTN: SMCAR-AEE	1
SMCAR-AES, BLDG. 321	1
SMCAR-AET-O, BLDG. 351N	1
SMCAR-CC	1
SMCAR-CCP-A	1
SMCAR-FSA	1
SMCAR-FSM-E	1
SMCAR-FSS-D, BLDG. 94	1
SMCAR-IMI-I (STINFO) BLDG. 59 PICATINNY ARSENAL, NJ 07806-5000	2
DIRECTOR US ARMY BALLISTIC RESEARCH LABORATORY ATTN: SLCBR-DD-T, BLDG. 305 ABERDEEN PROVING GROUND, MD 21005-5066	1
DIRECTOR US ARMY MATERIEL SYSTEMS ANALYSIS ACTV ATTN: AMXSY-MP ABERDEEN PROVING GROUND, MD 21005-5071	1
COMMANDER HQ, AMCCOM ATTN: AMSMC-IMP-L ROCK ISLAND, IL 61299-6000	1
COMMANDER ROCK ISLAND ARSENAL ATTN: SMCRI-ENM ROCK ISLAND, IL 61299-5000	1
DIRECTOR US ARMY INDUSTRIAL BASE ENGR ACTV ATTN: AMXIB-P ROCK ISLAND, IL 61299-7260	1
COMMANDER US ARMY TANK-AUTMV R&D COMMAND ATTN: AMSTA-DDL (TECH LIB) WARREN, MI 48397-5000	1
COMMANDER US MILITARY ACADEMY ATTN: DEPARTMENT OF MECHANICS WEST POINT, NY 10996-1792	1
US ARMY MISSILE COMMAND REDSTONE SCIENTIFIC INFO CTR ATTN: DOCUMENTS SECT, BLDG. 4484 REDSTONE ARSENAL, AL 35898-5241	2
COMMANDER US ARMY FGN SCIENCE AND TECH CTR ATTN: DRXST-SD 220 7TH STREET, N.E. CHARLOTTESVILLE, VA 22901	1
COMMANDER US ARMY LABCOM MATERIALS TECHNOLOGY LAB ATTN: SLCMT-IML (TECH LIB) WATERTOWN, MA 02172-0001	2

NOTE: PLEASE NOTIFY COMMANDER, ARMAMENT RESEARCH, DEVELOPMENT, AND ENGINEERING CENTER, US ARMY AMCCOM, ATTN: BENET LABORATORIES, SMCAR-CCB-TL, WATERVLIET, NY 12189-4050, OF ANY ADDRESS CHANGES.

TECHNICAL REPORT EXTERNAL DISTRIBUTION LIST (CONT'D)

	NO. OF COPIES
COMMANDER US ARMY LABCOM, ISA ATTN: SLCIS-IM-TL 2800 POWDER MILL ROAD ADELPHI, MD 20783-1145	1
COMMANDER US ARMY RESEARCH OFFICE ATTN: CHIEF, IPO P.O. BOX 12211 RESEARCH TRIANGLE PARK, NC 27709-2211	1
DIRECTOR US NAVAL RESEARCH LAB ATTN: MATERIALS SCI & TECH DIVISION CODE 26-27 (DOC LIB) WASHINGTON, D.C. 20375	1 1
COMMANDER AIR FORCE ARMAMENT LABORATORY ATTN: AFATL/MN EGLIN AFB, FL 32542-5434	1
COMMANDER AIR FORCE ARMAMENT LABORATORY ATTN: AFATL/MNF EGLIN AFB, FL 32542-5434	1
METALS AND CERAMICS INFO CTR BATTELLE COLUMBUS DIVISION 505 KING AVENUE COLUMBUS, OH 43201-2693	1

NOTE: PLEASE NOTIFY COMMANDER, ARMAMENT RESEARCH, DEVELOPMENT, AND ENGINEERING CENTER, US ARMY AMCCOM, ATTN: BENET LABORATORIES, SMCAR-CCB-TL, WATERVLIET, NY 12189-4050, OF ANY ADDRESS CHANGES.

DEPARTMENT OF THE ARMY
ARMAMENT RESEARCH, DEVELOPMENT AND ENGINEERING CENTER
BENÉT LABORATORIES, CCAC
US ARMY ARMAMENT, MUNITIONS AND CHEMICAL COMMAND
WATERVLIET, N.Y. 12189-4050

OFFICIAL BUSINESS

SMCAR-CCB-TL

BOOK RATE